The Nucleotide-Binding Site of the Sarcoplasmic Reticulum Ca−ATPase Is Conformationally Altered in Aged Skeletal Muscle†

Baowei Chen, Terry E. Jones, and Diana J. Bigelow*

Department of Molecular Biosciences, Biochemistry and Biophysics Section, Haworth Hall, University of Kansas, Lawrence, KS 66045-2106

Received May 17, 1999; Revised Manuscript Received August 9, 1999

ABSTRACT: Cellular conditions in senescent skeletal muscle have been shown to result in the loss of conformational stability of the sarcoplasmic reticulum (SR) Ca−ATPase. To identify underlying structural features of age-modified Ca−ATPase, we have utilized the fluorescence properties of protein-bound probes to assess both local and global structure. We find conformational changes that include an age-related decrease in the apparent binding affinity to high affinity calcium sites detected by fluorescence signals in both tryptophans within nearby membrane-spanning helices and fluorescein isothiocyanate (FITC) bound distally to Lys_{515} within the nucleotide-binding site. In addition, a substantial (80%) age-related increase in the accessibility to soluble quenchers of fluorescence of FITC is observed without concomitant changes in bimolecular quenching constants (k_q) for protein-bound IAEDANS, also within the nucleotide-binding domain, and tryptophans within the membrane. Using fluorescence resonance energy transfer to measure distances between IAEDANS and FITC across the nucleotide-binding domain, we find no significant age-related change in the mean donor−acceptor distance; however, significant increases are observed in the conformational heterogeneity of this domain, as assessed by the width at half-maximum (HW) of the distance distribution, increasing with age from 29.4 ± 0.8 Å to 42.5 ± 1.1 Å. Circular dichroism indicates that the average secondary structure is unaltered with age. Thus, these data suggest tertiary structural alterations in specific regions around the nucleotide-binding site rather than global conformational changes.

Both genetically transmitted alterations in protein sequence and posttranslational modifications have been shown to lead to conformational instability, misfolding, and enhanced propensity for aggregation of proteins that, in turn, can lead to cellular and organismal dysfunction. Specific examples where protein misfolding has been shown to be integral to pathologies include: β-amyloid in Alzheimer's disease, transthyretin in senile systemic amyloidosis, and prion protein in Creutzfeldt−Jacob disease (*1*−*4*). In addition, qualitatively similar conformational changes have been observed for a number of proteins in senescent mammalian tissues.

Similarly, the sarcoplasmic reticulum (SR)[1] Ca−ATPase in senescent skeletal muscle has been shown to be conformationally altered and less stable relative to this protein in young tissue (*5*, *6*). These characteristics may contribute to the prolonged relaxation times and muscle weakness observed in aging. Muscle relaxation is mediated by the SR Ca−ATPase that, in turn, mediates the rate-limiting resequestration of cytosolic calcium into the lumen of the SR, as a means to refill the internal stores for the next excitation−contraction event. Chronologically, one of the first contractile defects seen in aged muscle is a prolongation of the time required for relaxation that has been shown to be associated with decreased rates of calcium transport into the SR of some muscle types (*7*, *8*).

We have previously documented the age-related loss of functional and conformational stability of the Ca−ATPase in SR isolated from hindlimb skeletal muscle of the mammalian aging model, the Fischer 344 rat (*6*). From measurements of tryptic digestion in vitro, the Ca−ATPase isolated in intact SR membranes from senescent muscle exhibits increased initial rates of proteolysis relative to the Ca−ATPase from young muscle. The kinetics of this digestion suggests that ∼10% of the protein mass associated with the extramembranous cytoplasmic domain is more solvent exposed in aging. These conformational changes are associated with enhanced rates of Ca−ATPase inactivation, protein unfolding, and aggregation under conditions of mild heating, suggesting that the combination of age-modified Ca−ATPase and in vivo conditions where tissue may be heated to 41 °C by muscle activity may promote protein unfolding, aggregation, and loss of activity. Simulation of these age modifications by in vitro exposure of SR to reactive oxygen species suggests that oxidative modified forms of the Ca−ATPase accumulate in aging (*9*). However, in light of the multiple sites of oxidative modifications present in aged Ca−ATPase, we have sought to more precisely define conformationally

* To whom correspondence should be addressed. Telephone: (785) 864-3831. Fax: (785) 864-5321. E-mail: dbigelow@falcon.cc.ukans.edu.

† This work was supported by grants R01 AG12775 and P01 AG12993 from the National Institutes of Health.

[1] Abbreviations: FRET, fluorescence resonance energy transfer; SR, sarcoplasmic reticulum; IAEDANS, 5-[[2-[(iodoacetyl)amino]ethyl]-amino]naphthalene-1-sulfonic acid; FITC, fluorescein 5-isothiocyanate; POPOP, 1,4-bis[5-phenyl-2-oxazolyl]-benzene; SDS-PAGE, sodium dodecyl sulfate-polyacrylamide gel electrophoresis; MOPS, 3-(N-morpholino) propane-sulfonic acid.

10.1021/bi991125n CCC: $18.00
Published on Web 10/21/1999

altered regions utilizing site-directed fluorescent probes that provide measures of both local environment around fluorophores and molecular dimensions across the protein. From this work, focusing on the structure of the nucleotide binding domain, we find local tertiary structural changes around Lys_{515} within the nucleotide site and increased conformational heterogeneity of the nucleotide-binding domain without significant alterations in average secondary structure.

EXPERIMENTAL PROCEDURES

Materials. 5-[[2-[(iodoacetyl)amino]ethyl]amino]naphthalene-1-sulfonic acid (IAEDANS) was purchased from Molecular Probes (Eugene, OR); fluorescein 5-isothiocyanate, isomer I (FITC), 1,4-bis[5-phenyl-2-oxazolyl]-benzene (POPOP) were obtained from Sigma Chemical Co. (St. Louis). All other chemicals were of reagent grade.

Preparation of Rat Skeletal SR Membranes. Sarcoplasmic reticulum (SR) membranes were purified from the hind limb skeletal muscle of young (5 months), middle-aged (16 months), and old (26 months) Fischer strain 344 rat (obtained from Harlan−Sprague−Dawley; Indianapolis, IN) as described previously (*10*) with minor modifications (*11*). SR vesicles were suspended in a medium containing 0.3 M sucrose and 20 mM MOPS (pH 7.0) and stored at −70 °C. Protein concentrations were determined by the method of Lowry (*12*), using bovine serum albumin as a standard.

Assay of Enzymatic Activity. Calcium-dependent ATPase activity was assayed at 25 °C by colorimetric determination of the time dependence of the release of inorganic phosphate from vesicles made leaky to calcium by the addition of the ionophore A23187 (*13*). ATPase activity was measured in a medium containing 0.05 mg SR protein/mL, 0.1 M KCl, 5 mM $MgCl_2$, 4 μM A23187, 5 mM ATP, 25 mM MOPS (pH 7.0), 1 mM EGTA or 0.1 mM $CaCl_2$. Calcium-dependent ATPase activity was determined from subtracting the activity assayed in the presence of EGTA (basal activity) from the activity assayed in the presence of $CaCl_2$ (total ATPase activity).

Determination of Free Calcium Concentrations. Free calcium concentrations were determined from total ligand and EGTA concentrations, correcting for pH and ionic conditions (*14*).

Trypsin Digestion. SR vesicles labeled with either FITC or IAEDANS were subjected to mild tryptic digestion incubating 0.05 mg trypsin/mg SR protein for 20 min in 20 mM MOPS (pH 6.8), 80 mM KCl at 25 °C. The reaction was stopped by addition of soybean trypsin inhibitor (Type 1-S, Sigma) at an inhibitor/trypsin ratio of 2:1 (wt/wt).

Electrophoresis. Sodium dodecyl sulfate-polyacrylamide gel electrophoresis (SDS-PAGE) was performed according to the method of Laemmli (*15*). Fluorescence of IAEDANS or FITC associated with the polypeptides separated by SDS-PAGE was detected atop a UV light box (λ_{ex} = 366 nm) before staining with Comassie blue. Emission was monitored with a Corning 3-70 cutoff filter placed in front of the camera lens (Polaroid MP-4 Land Camera).

Labeling with Spectroscopic Probes. The Ca−ATPase was labeled with IAEDANS or FITC as previous described (*16*). Modification of the Ca−ATPase with IAEDANS was carried out in a medium of 20 mM MOPS (pH 6.8), 80 mM KCl, 1mM $CaCl_2$, 5 mM $MgCl_2$, and 4 mg of SR protein/mL for 30 min at 25 °C. The labeling medium included 10−100-fold excess IAEDANS (0.4−4 mM), ensuring complete modification of the reactive sulfhydryls. SR vesicles labeled with IAEDANS were separated from free probe by centrifugation at 100000*g* for 45 min followed by resuspension in sucrose buffer containing 0.3 M sucrose and 20 mM MOPS (pH 7.0), centrifuged again, and finally resuspended in sucrose buffer. The Ca−ATPase was labeled with FITC by incubation of SR with FITC for 10 min at 22 °C in a medium consisting of 10 mM Tris buffer (pH 9.2), 0.1 M KCl, 0.1 mM EGTA, 0.3 M sucrose. Unreacted label was removed by centrifugation of vesicles at 100000*g* for 45 min, the pellet was resuspended in sucrose buffer and centrifuged and finally resuspended in sucrose buffer. The stoichiometry of labeling for probes was determined in the medium of 1% SDS and 0.1 M NaOH for both probes using molar extinction coefficients of $\epsilon_{340} = 6100\ M^{-1}\ cm^{-1}$ and $\epsilon_{495} = 8.0 \times 10^4\ M^{-1}\ cm^{-1}$, for IAEDANS and FITC, respectively (*17*).

Steady-State Fluorescence Measurements. Fluorescence emission spectra were recorded with a FluoroMax-2 fluorometer (SPEX, Edison, NJ), using excitation and emission slits of 5 nm. In all cases, control samples (no fluorescent probes present) were used to determine the contribution of background fluorescence and/or scattered light to the observed spectra. Control samples demonstrated that these contributions were minimal (i.e., <6%).

Calcium-Dependent Fluorescence of FITC and Tryptophans. Changes in fluorescence due to calcium dependent changes in the environment of FITC bound to the Ca−ATPase or intrinsic tryptophans within the SR Ca−ATPase were measured by addition of small aliquots of a 0.2 M $CaCl_2$ stock into 3 mL of medium containing final concentrations of 40 μg SR/mL, 100 mM MOPS (pH 7.0), 80 mM KCl, 5 mM $MgCl_2$, and 1 mM EGTA. Free calcium concentrations were calculated based on total ligand and EGTA concentrations, correcting for pH and ionic conditions (*14*, *18*). Emission of FITC−SR was monitored at 518 nm with excitation at 495 nm, and emission of tryptophan was monitored at 333 nm with excitation at 290 nm.

Fluorescence Quenching Measurements. Protein conformational changes were assessed by changes in the accessibility of fluorophores to water-soluble quenchers of fluorescence. Acrylamide or KI was used as efficient quenchers of IAEDANS, FITC, and tryptophan fluorescence. Quenching of probes bound to the Ca−ATPase was measured by steady-state fluorescence intensities as a function of quencher concentration in 40 μg SR/mL, 20 mM MOPS (pH 7.0), 0.1 mM EGTA, and sufficient $CaCl_2$ to provide the desired concentrations of free calcium.

Frequency-Domain Fluorescence. Frequency domain data were measured using an ISS K2 frequency domain fluorometer described previously (*19*). The instrument was equipped with a Marconi signal generator (2022A & C) and ENI broad-band amplifiers (325LA and 403LA), which operate in conjunction with a Pockels cell to obtain intensity-modulated light from either a 300 W xenon arc lamp (ILC Technology PS300−1) or, alternatively, a CW argon ion laser equipped with extended UV capabilities (Coherent Innova 400/2/0.2, Santa Clara, CA).

Fluorescence lifetimes were determined using 351 nm for excitation of IAEDANS with an Oriel interference filter centered at 460 nm at 25 °C, using 1,4-bis[5-phenyl-2-oxazolyl]-benzene (POPOP) in absolute ethanol as a reference having a lifetime of 1.35 ns (*20*). The fluorescence lifetime of FITC was obtained at 488 nm for excitation using a Schott OG-530 cutoff filter and glycogen for relative standard (lifetime = 0). The frequency-domain data were analyzed by the method of nonlinear least-squares (*21*, *22*). The time-dependent decay I(t) of fluorescence is generally fitted to a sum of exponentials,

$$I(\mathrm{t}) = \sum \alpha_i e^{-t/\tau i} \qquad (1)$$

Where α_i is the preexponential factor and τ_i is the decay time, the intensity decay law is obtained from the frequency response of the amplitude-modulated light and is characterized by the frequency-dependent values of the phase shift and the extent of demodulation. The values are compared with the calculated values from an assumed decay law until a minimum of the squared deviation (χ_R^2) is obtained. Explicit expressions have been provided for calculation of α_i and τ_i.

Fluorescence Resonance Energy Transfer. The intensity decay for a fluorescence donor in the presence of an acceptor can provide information regarding both (1) the average distance between donor and acceptor and (2) the distribution of distances that reflects the static and dynamic conformational heterogeneity of the molecule to which donor and acceptor are bound. For example, for a single acceptor present at a distance r from a donor, the intensity decay (I_{DA}) is given by:

$$I_{DA}(r,t) = \sum_{i=1}^{n} (\alpha_{Di})^{-t/\tau_{DA}} \qquad (2)$$

where, individual decay times observed in the presence of an energy transfer acceptor are:

$$1/\tau_{DA_i} = 1/\tau_{D_i} + 1/\tau_{D_i}(R_0/r)^6 \qquad (3)$$

R_0 is the Förster critical distance that defines the distance where the efficiency of resonance energy transfer is 50% for a given donor−acceptor pair. R_0 is calculated as:

$$R_0 = (9.79 \times 10^3)(\kappa^2 n^{-4} Q J)^{1/6} \qquad (4)$$

where κ^2 is the orientation factor, n is the refractive index, Q is the quantum yield of the donor in the absence of the acceptor, and J is the spectral overlap integral (*20*). In our experiments, the quantum yield for IAEDANS−SR was determined using quinine bisulfate as a standard ($Q = 0.54$); the refractive index (n) was estimated to be 1.40 based on the refractive index measured for a 1 mg/mL solution of serum albumin (*23*). κ^2 was assumed to be 2/3, corresponding to random orientation between donor and acceptor dipoles, because of the range of conformations, the possibility of rotational diffusion, and the mixed polarization of the species (*24*). The use of $\kappa^2 = 2/3$ is not likely to result in significant error if donor and acceptor can adopt a range of conformations (*25*).

Modeling the distance distribution as a Gaussian probability ($P(r)$), the observed intensity decay is fit as:

$$I_{D_A} = \int_{r=0}^{\infty} P(r) \sum_{i=1}^{n} (\alpha_{D_i})^{-t/\tau_{Di} - (t/\tau_{Di})(R_0/r)^6} \, dr \qquad (5)$$

To recover $P(r)$ from the intensity decay, and minimize the number if parameters, a uniform Gaussian distribution of donor−acceptor distances is generally assumed:

$$P(r) = e^{-\frac{1}{2}\left(\frac{r - r_{av_2}}{\sigma}\right)} \qquad (6)$$

where r_{av} is the average donor−acceptor distance and σ is the standard deviation of the distribution. The width of the distribution is reported as the full width at half-maximum (HW), which is given by HW = 2.354σ. Additional details are available elsewhere (*26*).

Circular Dichroism. Spectra of SR proteins were measured using a Jasco J-710 spectropolarimeter with a temperature-jacketed spectral cell with a path length of 0.5 cm. CD spectra were collected from 205 to 260 nm (*27*).

RESULTS

Chemical Modification of the SR Ca−ATPase with IAEDANS and FITC. Conditions have been previously reported for the specific derivatization of the SR Ca−ATPase isolated from rabbit fast twitch muscle with both IAEDANS and FITC (*15*, *16*). These conditions result in modification of Lys_{515} by FITC (*28*) and of $Cys_{670,\ 674}$ by IAEDANS (*29*). Identical sequences around these sites in the Ca−ATPase of rat skeletal muscle (previously characterized as 85−90% fast-twitch (SERCA1) and 10−15% slow-twitch (SERCA2a) isoforms suggests that the same sites will be modified using these labeling conditions applied to SR isolated from the hindlimb skeletal muscle of Fischer 344 rats (*11*). This suggestion is confirmed by the following results. We find that derivatization of rat SR in the presence of excess IAEDANS results in the progressive incorporation of probe to a saturating level of 9.7 ± 0.4 nmol/mg of SR protein with the maintenance of >90% of the enzyme's activity. On the basis of the relative abundance of the Ca−ATPase in SR, this level is equivalent to approximately two moles of IAEDANS per Ca−ATPase polypeptide chain. For the experiments described in this study, we have used labeling conditions resulting in modification with approximately one mole of IAEDANS per mole of Ca−ATPase. On the other hand, labeling with FITC results in label saturation at 5.4 ± 0.8 nmol/mg of SR protein, corresponding to approximately one mol FITC/mol ATPase. Progressive modification with FITC correlates with a concomitant loss of Ca−ATPase activity, consistent with modification of a site that blocks access of nucleotide to the active site of the Ca−ATPase (*28*).

Probe specificity was assessed after electrophoretic separation of SR proteins (Figure 1). Fluorescence of both IAEDANS and FITC is associated primarily with the 100 kDa Ca−ATPase protein band and with the B tryptic fragment (Ala_{506}−Lys_{1001}) consistent with the sites of modification previously reported for the rabbit skeletal muscle enzyme (*28*, *29*). Neither labeling stoichiometries nor

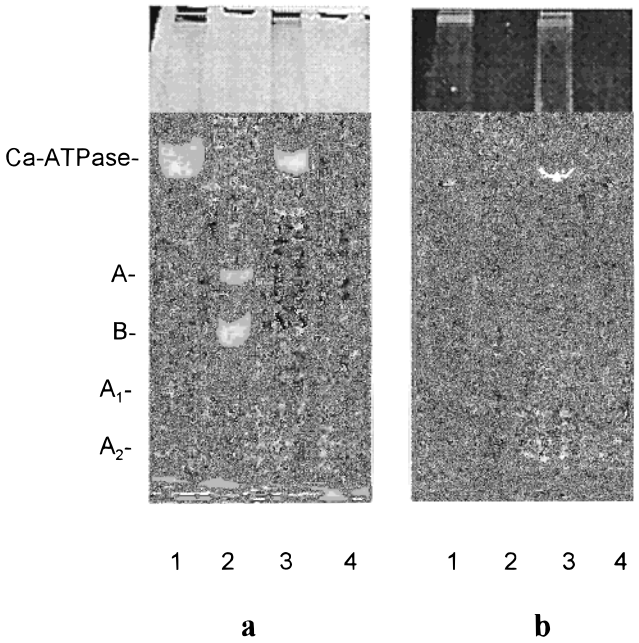

FIGURE 1: IAEDANS and FITC modification of the SR Ca−ATPase. SR vesicles were labeled with IAEDANS (lanes 1 and 2), and with FITC (lanes 3 and 4) before separation of protein on 7.5% SDS-PAGE. The left panel (a) depicts Coomassie blue staining before (lanes 1 and 3) and after (lanes 2 and 4) mild digestion with trypsin (see Experimental Procedures). The right panel (b) depicts protein and peptide-associated fluorescence from the same samples. Fluorescence was detected using a Corning 3-70 cutoff filter before staining with Coomassie blue. A and B indicate tryptic fragments resulting from the initial cleavage at R505; A_1 and A_2 indicate tryptic fragments derived from further cleavage of A at R198.

specificities of either probe differ for preparations isolated from rats of different ages (data not shown).

Calcium-Dependent Structural Transitions. The fluorescence of FITC covalently bound to Lys_{515} within the nucleotide site of the Ca−ATPase has been shown to be sensitive to calcium binding at the distal transmembrane sites within the Ca−ATPase, exhibiting a 8−9% decrease of fluorescence intensity upon calcium binding (*30*, *31*). In this study, we have compared these calcium-dependent structural transitions in SR isolated from skeletal muscle of young with those from aged animals (Figure 2A). All data were fit using the Hill equation resolving the half-saturation calcium concentrations ($K_{1/2}$) and Hill coefficients (n_H). FITC quenching induced by calcium binding occurs at lower ($p<0.05$) free calcium concentrations for SR membranes isolated from young skeletal muscle ($K_{1/2} = 1.5 \pm 0.1$ μM) relative to that observed from aged skeletal muscle ($K_{1/2} = 2.4 \pm 0.2$ μM). In contrast, the Hill coefficients (1.9 ± 0.2 and 2.1 ± 0.3 for young and old samples, respectively) do not significantly differ. Neither is the total extent of the fluorescence change (8−9%) different with age. Another structural transition in response to high affinity calcium binding was examines, i.e., the 4−5% enhancement of intrinsic fluorescence that originates from some or all of the 12 tryptophans within membrane-spanning helices (*32*). The same relative shift to higher calcium concentrations is observed for this fluorescence signal for the Ca−ATPase from aged muscle (Figure 2B). Recovered K_2 values of 1.2 ± 0.1 μM and 1.7 ± 0.1 μM for young and aged samples, respectively, are significantly different ($p<0.1$), with no change in Hill coefficients

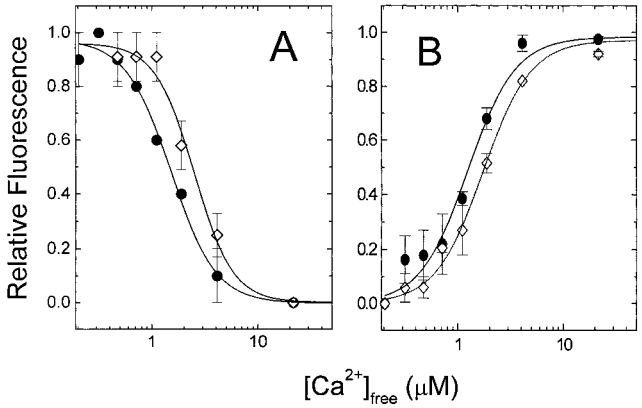

FIGURE 2: Calcium dependence of relative fluorescence changes entailing (panel A) the quenching of fluorescence of bound FITC and (panel B) enhancement in the fluorescence of intrinsic tryptophans within the SR Ca−ATPase from skeletal muscle of young (5 mo) adult (●) and aged (26 mo) (◇) Fischer 344 rats. Relative fluorescence is calculated from $(F - F_{min})/(F_{max} - F_{min})$, where F is fluorescence intensity under any experimental conditions, F_{max} and F_{min} are maximum and minimum intensities, respectively. These measurements were carried out in a buffer consisting of 40 μg SR/mL, 100 mM MOPS (pH 7.0), 80 mM KCl, 5 mM $MgCl_2$, 1 mM EGTA. Each data point represents the mean of three measurements from SR isolated from young and aged muscle where probe stoichiometries were 6.2 ± 0.4 and 6.4 ± 0.8 nmol FITC/mg SR protein, respectively. Emission of FITC−SR was measured at 518 nm with excitation at 495 nm; emission of tryptophan was monitored at 333 nm with excitation at 290 nm.

or total fluorescence changes. Thus, the age-related decrease in the apparent calcium affinity, i.e., either calcium-binding itself, or calcium-dependent activation steps, are manifested in structural changes at spatially distal sites within the Ca−ATPase.

Solvent Accessibility of Intrinsic and Extrinsic Fluorophores. We have assessed possible changes in the local environment around IAEDANS, FITC, and tryptophans with respect to the extent to which these groups are buried within the protein structure measuring the accessibility of these fluorophores to water-soluble quenchers of fluorescence. Increased solvent accessibility is suggested from the increasing slopes of the Stern−Volmer plots (K_{SV}) of iodide quenching of protein-bound FITC with age (Figure 3A). Since changes in the quenching can also result from changes in probe lifetime, which alter the time available for collisional quenching, fluorescence lifetimes of FITC were measured in order to derive the bimolecular quenching constants ($k_q = K_{sv} \times \tau^{-1}$), as a true measure of solvent accessibility (Table 1). Comparison of the bimolecular quenching constant (k_q) of FITC to KI for the SR Ca−ATPase from aged muscle relative to those from middle-aged and young muscle indicates a progressive increase up to nearly 1.8-fold in the solvent accessibility of this fluorophore within the nucleotide site. However, in all cases, the solvent accessibility of protein-bound FITC remains less than that of FITC free in solution, indicating only partial loss of structure around Lys_{515}. In contrast, IAEDANS, covalently bound to a distal site within the B tryptic fragment of the Ca−ATPase, exhibits no significant changes in solvent accessibility to either KI or the neutral quencher, acrylamide, with age of the animal (Figure 3B). Similarly, quenching of intrinsic tryptophan fluorescence was unchanged with age (Figure 3B). Thus, these results, in combination with the observation that there

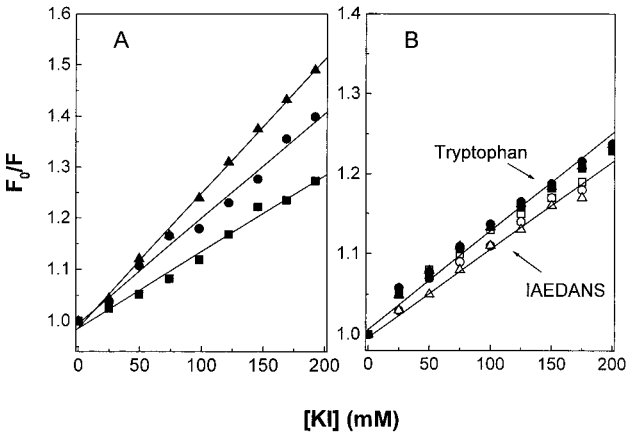

FIGURE 3: Accessibility to quenching by iodide of fluorophores bound to the Ca−ATPase. Quenching was measured from fluorescence intensities of (panel A) bound FITC, or (panel B) bound IAEDANS (open symbols) or intrinsic tryptophans (solid symbols) (panel B) as fluorescence intensities (F) relative to unquenched samples (F_0) at various KI concentrations. Samples consisted of 40 μg SR/mL and 20 mM MOPS (pH 7.0), 0.1 mM EGTA, 56.2 μM $CaCl_2$ ($[Ca^{2+}]_{free}$ = 0.5 μM, and sufficient KCl (up to 0.2 M) to maintain a constant ionic strength in solution. SR from 5 month (squares), 16 month (circles), and 26 month-old (triangles) animals was derivatized with 4.3 ± 0.1 nmol FITC/mg SR or 5.8 ± 0.1 nmol IAEDANS/mg SR. Fluorescence was measured at 518 nm with excitation at 495 nm for FITC, at 480 nm with excitation at 340 nm for IAEDANS, and 333 nm with excitation at 290 nm for tryptophan. Data points represent the mean of two FITC and IAEDANS or three tryptophan measurements.

Table 1: Age-Related Differences in the Solvent Accessibility of FITC Bound to the Ca−ATPase in SR[a]

sample	K_{sv} (M^{-1})[b]	$<\tau>$ (ns)[c]	k_q (10^{-9} M^{-1} s^{-1})[d]
FITC-SR			
5 months	1.35 (±0.10)	3.34 (±0.03)	0.40 (±0.03)
16 months	1.93 (±0.12)[e]	3.49 (±0.12)	0.54 (±0.04)
26 months	2.42 (±0.14)[e]	3.36 (±0.03)	0.72 (±0.04)
FITC	4.08 (±0.40)	3.11 (±0.04)	1.31 (±0.05)

[a] SR isolated from skeletal muscle of various aged rats was derivatized by FITC under conditions described in Experimental Procedures that specifically modifies the Ca−ATPase (FITC-SR), or lysine alone was derivatized (FITC) before quenching with iodide or lifetime measurements were made. These measurements were made under the buffer conditions described in Figure 3. [b] K_{sv}, the slope of the Stern−Volmer plot, was obtained from the relationship $F_0/F = 1.0 + K_{sv}(Q)$, where F_0 and F is the fluorescence intensity in the absence or presence of added quenchers, Q is the quencher concentration; Stern−Volmer plots are as in Figure 3. [c] Fluorescence lifetimes ($<\tau>$) are expressed as $\sum f_i \tau_i$. [d] k_q is the bimolecular quenching constant, where $k_q = K_{sv} <\tau>^{-1}$. Errors (in parentheses) represent the mean of two measurements each from two individual animals. [e] Indicates significance calculated from Student's t-test of $p<0.01$ relative to samples from 5 month animals.

is an age-related loss in sensitivity to calcium binding, suggest that while the environment around tryptophans in membrane spanning helices undergoes changes with age, these changes do not affect their position with respect to the aqueous medium.

Fluorescence Resonance Energy Transfer Between IAEDANS and FITC, and Distance Distribution Analysis. The modification of the Ca−ATPase with both IAEDANS and FITC provides a sensitive donor−acceptor pair for the estimation of molecular distances across the nucleotide-binding domain from fluorescence resonance energy transfer (FRET) measurements. Therefore, we have used frequency domain measurements of lifetimes of bound IAEDANS in the presence and absence of FITC in order to recover information regarding the extent of heterogeneity in donor−acceptor distances and thus conformations within the cytoplasmic domain of the Ca−ATPase. From the donor's emission, the phase lag and demodulation of intensity-modulated light relative to the excitation was measured at 20 different frequencies between 2 and 100 MHZ (Figure 4). The intensity decay of both IAEDANS−SR and IAEDANS−FITC−SR are adequately described as the sum of three exponentials, as shown by the random distribution of the weighted residuals and the relative reduction in chi-squared values (Table 2). A near 60-fold improvement in the goodness of fit (i.e., χ^2_R) for a model involving three-exponentials relative to the two-exponential model is observed, indicating that three-exponential model is statistically justified. Fitting to a four-exponential model does not significantly improve the fit. The relative shifts in demodulation and phase of IAEDANS toward higher frequencies in the presence of FITC is indicative of a decreased lifetime as a result of FRET that can also be seen from the lifetime data (Table 2).

These data has also been modeled as a Gaussian distribution of donor−acceptor distances that reflects the degree of static or dynamic disorder resulting from either multiple conformations or structural fluctuations of the Ca−ATPase polypeptide chain (*33*). From this analysis, we find the average recovered donor−acceptor distance (r_{av}) between IAEDANS and FITC is not significantly different as a result of age as evidenced by overlapping error surfaces within one standard deviation (Figure 5C). In contrast, the extent of conformational heterogeneity progressively increases with age as evidenced by the width at half-maximum (HW) of the distance distribution with the greatest change occurring between 16 and 26 months of age (Figure 5, Table 3).

These age-related conformational modifications were also compared with those produced by the global unfolding induced by the denaturant urea. Like aging, exposure to urea results in only minimal changes in the average distance (r_{av}) between IAEDANS and FITC, but substantial increases in the HW of the distance distribution. As indicated by the arrows in Figure 6, the extent of the increased HW occurring in middle-aged and senescent muscle corresponds to that produced by in vitro treatment with 1.4 M and 2.7 M urea, respectively. However, unlike age modifications, exposure to urea results in substantial inactivation of the Ca−ATPase (approximately 80% at 3 M urea). In contrast, aging results in little or no loss of activity under optimal assay conditions; however, a loss of stability is observed (*11*, *35*).

Circular Dichroism Measurements. Possible age-related changes in secondary structure of the Ca−ATPase, were assessed with circular dichroism (CD) spectroscopy. In view of its age-related loss of conformational stability, further purification of the Ca−ATPase with its requisite removal from the stabilizing influence of the SR membrane would likely result in artifactual results. Therefore, the apparent α-helical content was estimated from CD of native SR membranes in which the Ca−ATPase comprises the major (>50%, based on gel densitometry), but not only, component (Figure 7). CD spectra were measured from 206 to 260 nm at 1 nm intervals for SR vesicles isolated from the skeletal

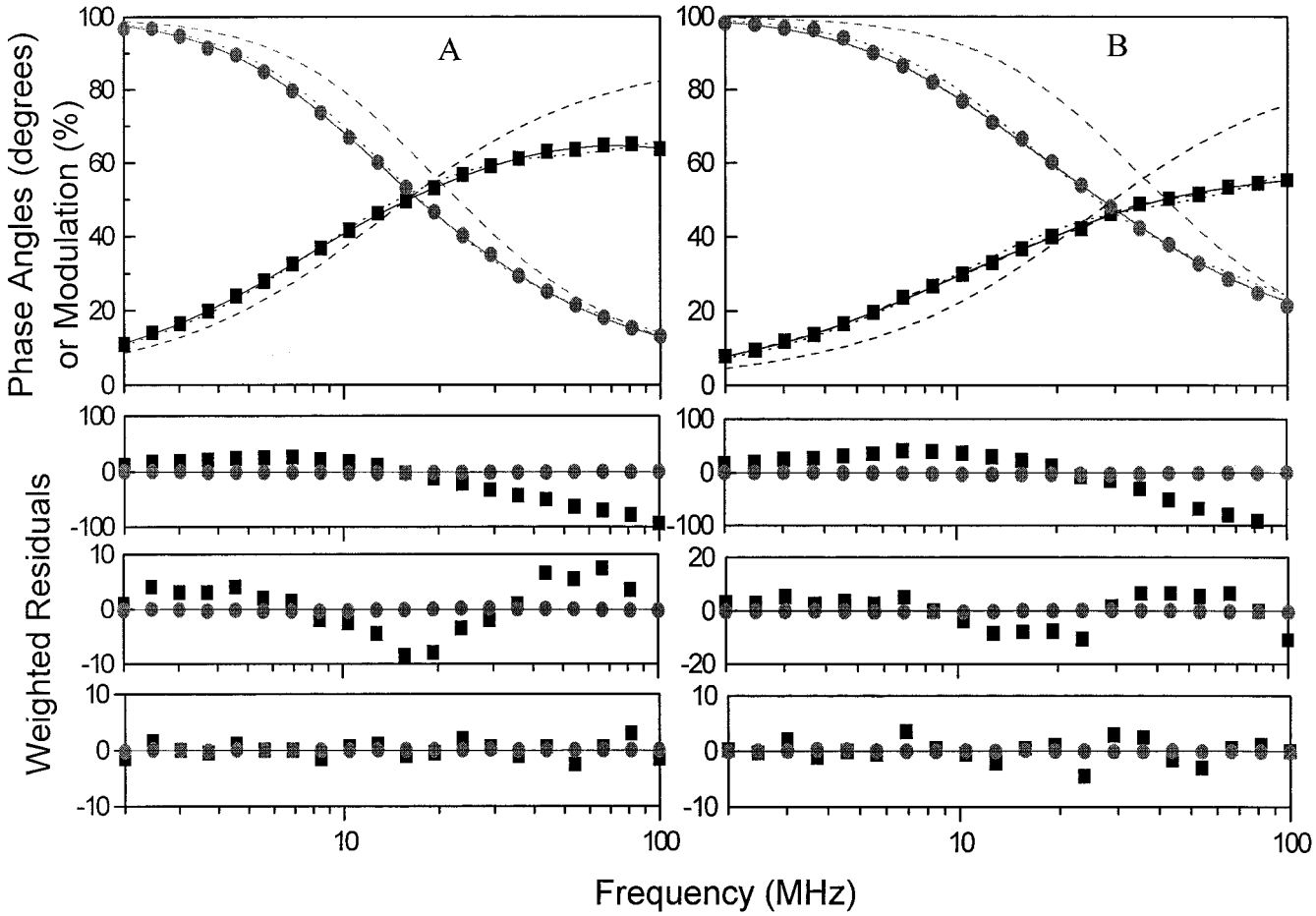

FIGURE 4: The frequency response of the emission of IAEDANS bound to the Ca−ATPase of SR isolated from 5 month animals at 25 °C. Data are shown for IAEDANS−SR (left panel) and IAEDANS−FITC−SR (right panel) for the differential phase angle (■) and modulation (●). The fits correspond to one (dashed line), two (dotted line), and three (solid line) exponential components. Weighted residuals (phase and modulation) are shown below the frequency domain data, and from top to bottom, correspond to one-, two-, and three-exponential fits to the data. The weighted residuals correspond to the difference between the experimental data and the calculated fit divided by the standard error of the individual measurements, which was assumed to be 0.20 and 0.005 for phase and modulation data, respectively. The reduced chi-squared (χ^2_R) values for fits of IAEDANS−SR are 964, 16.9, and 1.3 for one-, two-, and three-exponential models, respectively. Chi-squared values for fits of IAEDANS−FITC−SR are 1410, 23.8, and 2.9 for one-, two-, and three exponential models, respectively. Lifetime measurements were made in medium contained 100 μg SR/mL, 20 mM MOPS (pH 6.8), 80 mM KCl, 5 mM $MgCl_2$, 0.5 mM EGTA. Probe stoichiometries were 5.7 ± 0.1 nmol IAEDANS/mg SR or 2.3 ± 0.3 nmol FITC/mg SR.

Table 2: Lifetime Data for IAEDANS-Modified SR Ca−ATPase[a]

sample	α_1	τ_1 (ns)	α_2	τ_2 (ns)	α_3	τ_3 (ns)	$\Sigma\alpha_i\tau_i$ (ns)	χ^2_R
IAEDANS-SR								
5 months	0.228	19.3	0.175	6.56	0.597	0.570	5.89	2.1
	(0.009)	(0.5)	(0.025)	(0.62)	(0.016)	(0.181)	(0.30)	
16 months	0.280	18.1	0.141	4.79	0.579	0.479	6.02	2.2
	(0.006)	(0.3)	(0.001)	(0.28)	(0.006)	(0.053)	(0.04)	
26 months	0.281	18.9	0.179	6.34	0.540	0.64	6.79	2.7
	(0.025)	(0.1)	(0.012)	(0.46)	(0.012)	(0.098)	(0.56)	
IAEDANS-FITC-SR								
5 months	0.117	16.0	0.217	4.87	0.666	0.532	3.28	4.4
	(0.009)	(0.8)	(0.024)	(0.81)	(0.03)	(0.223)	(0.64)	
16 months	0.137	14.8	0.200	4.21	0.663	0.463	3.17	3.3
	(0.009)	(0.2)	(0.010)	(0.04)	(0.019)	(0.055)	(0.17)	
26 months	0.136	15.9	0.216	4.91	0.648	0.548	3.58	3.3
	(0.010)	(1.0)	(0.025)	(0.77)	(0.016)	(0.208)	(0.40)	

[a]Experimental conditions: 100 μg SR/mL, 20 mM MOPS (pH 6.8), 80 mM KCl, 5 mM $MgCl_2$, and 0.5 mM EGTA at 25 °C with excitation at 351 nm using an Oriel interference filter centered at 460 nm. The probe stoichiometry of the IAEDANS-labeled sample was 5.7 ± 0.1 nmol/mg SR, that for FITC was 2.3 ± 0.3 nmol/mg SR. Average amplitudes (α_i) and lifetimes (τ_i) were obtained from three-exponential fits to frequency domain data collected for donor only and donor−acceptor SR Ca−ATPase isolated from different aged skeletal muscle (5 months, 16 months, and 26 months). Errors (shown in parentheses) are the mean of three measurements.

muscle of 6, 17, and 26 month old Fischer 344 rats. The resulting spectra show no age-related changes, detectable within the experimental variability of 3%, in average secondary structure of SR proteins. In contrast, exposure of SR to urea results in a substantial loss in secondary structure as evidenced by the spectrum of SR in 3 M urea, and the

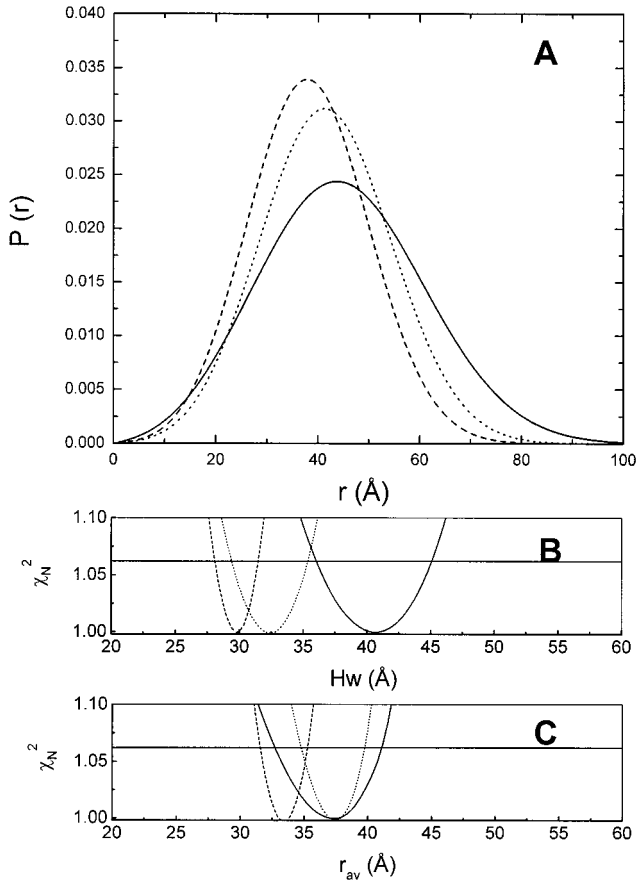

FIGURE 5: Distribution of distances from IAEDANS bound to Ca−ATPase to FITC (panel A) and normalized chi-squared (χ^2_N) error surfaces for the width at half-maximum (HW) (panel B) or the average donor−acceptor distance (r_{av}) recovered for protein-bound probes. Lines in panels B and C indicate one standard deviation. The samples were measured under buffer conditions as in Figure 4. SR vesicles were isolated from a 5 month (dashed lines), 16 month (dotted lines), or 26 month-old (solid lines) rat.

Table 3: Distance Distribution Analysis of Resonance Energy Transfer Between IAEDANS and FITC Bound to the Ca−ATPase[a]

sample	E	R_0 (Å)	r_{av} (Å)	HW (Å)	χ_R^2
5 months	0.44 ± 0.09	47 ± 3	33.7 ± 0.8	29.4 ± 0.8	4.4
16 months	0.47 ± 0.03	47 ± 3	38.8 ± 1.1	32.0 ± 1.2	4.3
26 months	0.47 ± 0.07	48 ± 3	38.3 ± 1.2	42.5 ± 1.1	1.5

[a] Experiments were carried out at 25 °C with excitation at 351 nm using an Oriel interference filter centered at 460 nm. The medium buffer contained 100 μg modified SR/mL, 20 mM MOPS (pH 6.8), 80 mM KCl, 5 mM $MgCl_2$, 0.5 mM EGTA. The errors associated with E% are propagated using the equation: $\sigma^2_x/x^2 = a^2/u^2 + b^2/v^2$ (*34*). r_{av} and HW values are derived from a global fitting of data from two individual animals for each age group.

increases in molar ellipticity at 222 nm induced by up to 4 M urea shown in Figure 7B. That urea so significantly alters the secondary structure of SR proteins while age does not further suggests that age modifications of Ca−ATPase structure are distinct from those due to global unfolding.

We also specifically examined the Ca−ATPase with respect to any age-related differences in its sensitivity to urea-induced unfolding, comparing calcium-dependent ATPase activities of SR isolated from young adult with that from senescent animals (Figure 8). The urea-induced loss of Ca−ATPase activity occurs with a half-point of approximately 2 M without significant age-related differences.

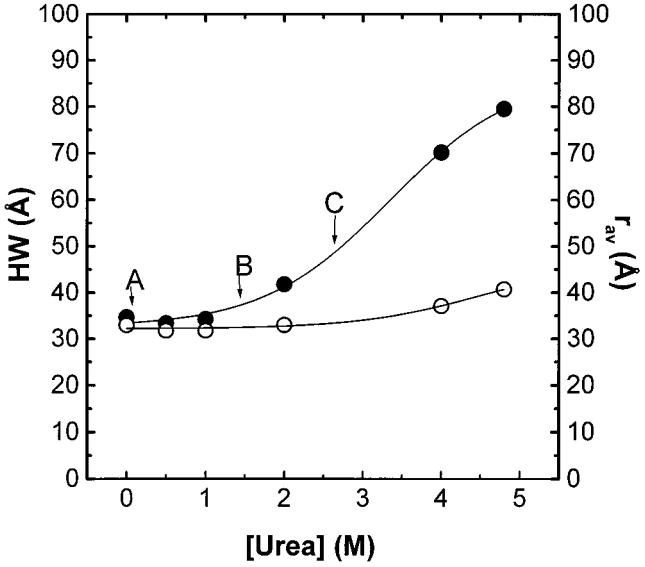

FIGURE 6: Effect of urea on average distance (r_{av}) (○) and width at half-maximum (HW) (●) in distribution of distances from IAEDANS to FITC. Arrows indicate r_{av} and HW obtained from similar measurements of the Ca−ATPase (in the absence of urea) corresponding to SR isolated from 5 month (A), 16 month (B), and 26 month (C) Fischer 344 rats (see Table 3). The medium contained 100 μg SR (isolated from 5 month animals)/mL, 20 mM MOPS (pH 6.8), 80 mM KCl, 5 mM $MgCl_2$, and 0.5 mM EGTA, and probe stoichiometries were 3.0 ± 0.1 nmol IAEDANS/mg SR or 3.8 ± 0.2 nmol FITC/mg SR.

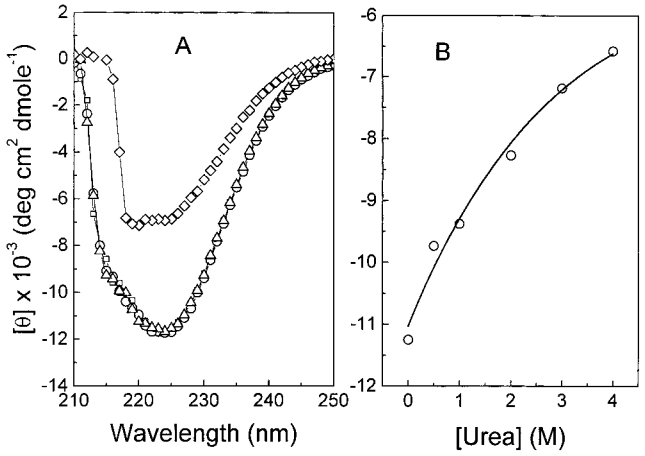

FIGURE 7: Panel A: Circular dichroism spectra of native SR vesicles isolated from 6 (□), 17 (○), and 26 (△) month Fischer 344 rats compared with the spectrum from SR isolated from 6 month animals treated with 3 M urea (◇). Panel B: The effect of urea concentration on ellipticity values at 222 nm. Molar ellipticity was measured for 0.04 mg/mL SR suspended in 20 mM MOPS (pH 6.8), 80 mM KCl, 5 mM $MgCl_2$, and 0.5 mM EGTA and calculated based on average residue molecular mass of 115 Da. Data points represent the mean of three measurements.

DISCUSSION

Summary of Results. In the present study, we have identified conformational alterations of the SR Ca−ATPase associated with aging. The differential alterations in solvent exposure of fluorophores, FITC and IAEDANS indicate structural changes that are localized around Lys_{515} in the nucleotide site without perturbation at the distal Cys $_{670,674}$ (Figure 3). Moreover, the overall conformation of the nucleotide binding domain is unaltered as indicated by the mean distance between IAEDANS at $Cys_{670,674}$ and FITC

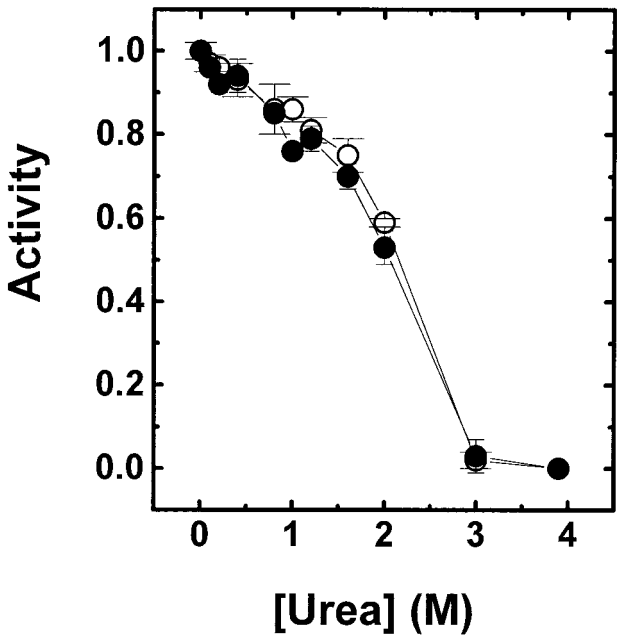

FIGURE 8: Sensitivity of the Ca−ATPase to urea-induced denaturation. Calcium-dependent ATPase activity was measured as described in Experimental Procedures for SR vesicles isolated from the skeletal muscle of 5 month (○) or 26 month (●) Fischer 344 rats incubated with the specified (final) concentration of urea. Ca−ATPase activity is normalized relative to the activity measured in the absence of urea, i.e., 2.27 ± 0.02 μmol Pi/mg/min. Data points represent the means ± S.E.s of two activity measurements each for SR membranes isolated from three animals each.

(Figure 5). However, the structural changes around Lys_{515} are likely to provide a substantial contribution to the dramatic increases observed in the conformational heterogeneity of the nucleotide-binding domain. In addition, residues within transmembrane helices show subtle modifications with age as demonstrated by the loss of structural coupling between calcium binding and tryptophan fluorescence (Figure 2). The lack of any detectable change in solvent accessibility of tryptophans in membrane spanning peptides implies that the structural changes that occur are such that they do not affect the disposition of the transmembrane helices with respect to the lipid bilayer. Together, these results are consistent with previous work demonstrating age-related increases in tryptic sensitivity of an estimated 10% of the cytoplasmic protein mass that suggest localized exposure of buried groups (*11*). In the present study, we also find that the average secondary structure is not altered by the sum of structural changes in either transmembrane or cytoplasmic domains (Figure 7). Previous rotational diffusion measurements utilizing protein bound spin labels have demonstrated that neither does aging alter the association state of the Ca−ATPase (*6*).

We have contrasted the protein modifications resulting from age with those produced by a nonselective perturbant, urea (Figure 6, 7). Urea acts on soluble proteins as a nonspecific denaturant inducing global unfolding and likely induces a similar type of unfolding within the large cytoplasmic domain of the Ca−ATPase which represents approximately 60% of the protein's mass. Urea does not solubilize SR vesicles or perturb the fluorescence of membrane bound fluorophores indicating that despite denaturation of the cytoplasmic domain, these unfolded peptides remain tethered to structurally unperturbed membrane-spanning peptides (*35*). That the cytoplasmic domain unfolds in similar fashion as soluble proteins is suggested by the observation that urea titration induces changes in fluorescence signals associated with the Ca−ATPase that exhibit sharp transitions characteristic of highly cooperative unfolding processes and having free energies of denaturation (ΔG_D) (~4 kcal mol^{-1} at room temperature) typical of the denaturation of soluble proteins (*35*). Similarly, guanidinium chloride, another chaotrope, has been shown to produce unfolding specifically of an extramembranous domain of the Ca−ATPase (*36*). Thus, the contrast between structural effects on the Ca−ATPase of a known global process with that of age modification emphasizes their differences. For example, while 2.75 M urea simulates the effects of age on the distribution and average of molecular distances between IAEDANS and FITC, its effects on other structural parameters are quite distinct (Figure 6). For example, this extent of unfolding induced by urea results in almost complete (80%) inactivation of the Ca−ATPase, significant (12%) loss of secondary structure (Figure 7), and a 20% loss of total tryptophan fluorescence signal. All of these are consistent with extensive effects on Ca−ATPase structure and function in contrast to undetectable changes of secondary structure, tryptophan fluorescence, and enzyme activity with age.

Underlying Basis for Age-Related Conformational Modifications. A number of hypotheses have been proposed, relevant to the Ca−ATPase, regarding the underlying mechanism for alterations in conformational stability and function with aging. These include: (1) changes in the cellular environment which allow partial unfolding of proteins which in their native form, although transiently stable, may not be at the minimum free energy of folding; (2) posttranslational modifications of the Ca−ATPase protein; and (3) especially in the case of membrane proteins, changes in lipid composition (*37*). The latter factor has potential to be an important factor for the Ca−ATPase whose activity has been shown to be sensitive to the physical properties of the surrounding lipid bilayer (*38*−*41*). However, previously we have demonstrated that with age the SR lipid bilayer maintains physical characteristics that provide for optimal transport activity and stability of the Ca−ATPase despite measurable changes in fatty acyl chain composition (*42*).

Therefore, in view of the preponderance of oxidative modifications that are associated with the Ca−ATPase from senescent muscle, we favor the hypothesis that posttranslational oxidative modifications are the most likely basis for the observed age-related changes in the functional stability of the Ca−ATPase. And, a causal relationship is suggested by the simulation of age-related differences in functional stability, increased propensity for aggregation, and increased proteolytic susceptibility by mild oxidation of the Ca−ATPase by exposure to low concentrations of reactive oxygen species (*9*). Chemical analysis has revealed the accumulation of numerous oxidative modifications to the Ca−ATPase with age. These include the accumulation of substantial amounts (stoichiometric with the Ca−ATPase) of modified cysteines and, specifically for SERCA2a, tyrosines (*43*). Additionally, smaller increases in other amino acid modifications are observed that are cumulatively detected as their aldehydic (carbonyl) compounds (*9*). In the absence of the complete identification of the multiple oxidatively modified amino acid residues modified within the primary sequence of the Ca−ATPase, the detection of structural changes in

aging suggests protein regions relevant to functional stability.

While the specific sites of oxidatively modified cysteines have not been identified, likely candidates might include Cys_{498} or Cys_{525}, since these cysteines lie within sequences predicted to fold as α-sheets just N-terminal and C-terminal, respectively, to the predicted α-helix containing the FITC-modified Lys_{515} (*44*); similarly, in SERCA2a, a nearby tyrosine (Y_{497}) may be involved. Future analysis should focus on these sites. Definition of the pattern of chemical modifications and structural consequences will provide an oxidative "footprint" that will permit identification of the cellular reactive oxygen species that are responsible for age-related accumulation of oxidized protein.

Physiological Relevance of Ca−ATPase Structural Changes. In this and previous studies, we have documented the age-related loss of conformational stability of the SR Ca−ATPase isolated from the both fast- and slow-twitch muscles comprising the hindlimb muscles of the Fischer 344 rat (*6*, *9*, *44*). Without any significant decrease in either ATP hydrolytic activity or calcium transport activities, as assayed under optimal conditions, the Ca−ATPase in SR isolated from senescent muscle undergoes a more rapid inactivation with mild in vitro heating which is accompanied by increased noncovalent aggregation and unfolding (*6*). We speculate that, with age, a larger fraction of Ca−ATPase polypeptides undergo this inactivation process in vivo during moderate to extensive muscle activity when tissue temperatures become elevated. Skeletal muscle is unique in its ability to undergo temperature elevations with activity and comprises the major source of nonshivering thermogenesis in animals without brown fat (*45*−*47*). Thus, in senescence an increased fraction of less active Ca−ATPase molecules in the SR is likely to contribute to reduced calcium transport activity with a concomitant prolongation of muscle relaxation times. That decreased activity in SR isolated from aged animals is not observed may relate to extensive aggregation of these inactive species, which precludes copurification with active Ca−ATPase. In addition, the fast-twitch (SERCA1) and slow-twitch (SERCA2a) isoforms of the Ca−ATPase appear to be differentially affected by age (*8*, *44*). Using SR isolated from selected fast or slow-twitch muscles, we find that SERCA2a exhibits more dramatic decreases in function with age, which may be related to different posttranslational modifications with age relative to that of SERCA1 (*44*). Therefore the structural changes we observe in this study may be a reflection of predominantly changes of SERCA2a. Distinguishing the precise origin of age-related structural changes of the Ca−ATPase will require the ability to purify (or enrich) vesicles with each isoform in sufficient amounts for structural studies.

ACKNOWLEDGMENT

We sincerely thank Dr. Hongye Sun for helpful discussions and his assistance with the measurement of frequency domain fluorescence spectroscopy.

REFERENCES

1. Kelly, J. W., and Lansbury, P. T. (1994) *Amyloid 1*, 186−205.
2. Come, J. H., and Lansbury, P. T., Jr. (1994) *J. Am. Chem. Soc. 116*, 4109−4110.
3. Nguyen, J., Baldwin, M. A., Cohen, F. E., and Prusiner, S. B. (1995) *Biochemistry 34*, 4186−4192.
4. Kelly, J. W. (1996) *Curr. Opin. Struct. Biol. 6*, 11−17.
5. Gafni, A., and Yuh, K. C. (1989) *Mech. Aging Dev. 49*, 105−117.
6. Ferrington, D. A., Jones, T. E., Qin, Z., Miller-Schlyer, M., Squier, T. C., and Bigelow, D. J. (1997) *Biochim. Biophys. Acta 1330*, 233−247.
7. Larsson, L., and Salviati, G. (1989) *J. Physiol*, *419*, 253−264.
8. Narayanan, N., Jones, D. L., Xu, A., and Yu, J. C. (1996) *Am. J. Physiol. 271*, C1032−C1040.
9. Viner, R. I., Ferrington, D. A., Aced, G. I., Miller-Schlyer, M., Bigelow, D. J., and Schoneich, C. (1997) *Biochim. Biophys. Acta 1329*, 321−335.
10. Fernandez, J. L., Rosemblatt, M., and Hidalgo, C. (1980) *Biochim. Biophys. Acta 599*, 552−568.
11. Ferrington, D. A., Reijneveld, J. C., Bär, P. R., and Bigelow, D. J. (1996) *Biochim. Biophys. Acta 1279*, 203−213.
12. Lowry, O. H., Rosebrough, N. J., Farr, A. L., and Randall, R. J. (1951) *J. Biol. Chem. 193*, 265−275.
13. Lanzetta, P. A., Alvarez, L. J., Reinach, P. S., and Candia, D. A. (1979) *Anal. Biochem. 100*, 95−97.
14. Fabiato, A. (1988) *Methods Enzymol. 157*, 378−417.
15. Laemmli, U. K. (1970) *Nature 227*, 680−685.
16. Squier, T. C., Bigelow, D. J., Garcia de Ancos, J., and Inesi, G. (1987) *J. Biol. Chem. 262*, 4748−4754.
17. Bigelow, D. J., and Inesi, G. (1991) *Biochemistry 30*, 2113-2125.
18. Fabiato, A., and Fabiato, F. (1979) *J. Physiol. (Paris) 75*, 463−505.
19. Yao, Y., Schoneich, Ch., and Squier, T. C. (1994) *Biochemistry 33*, 7797−7810.
20. Lakowicz, J. R. (1983) *Principles of Fluorescence Spectroscopy*, Plenum Publishing Corp., New York.
21. Gratton, E., Lakowicz, J. R., Maliwal, B., Cherek, H., Laczko, G., and Limkeman, M. (1984) *Biophys. J. 46*, 479−486.
22. Lakowicz, J. R., and Keating-Nakamoto, S. (1984) *Biochemistry 23*, 3013−3021.
23. Fairclough, R. H., and Cantor, C. R. (1978) *Methods Enzymol. 48*, 347−379.
24. Haas, E., Katchalski-Katzir, E., and Steinberg, I. Z. (1978) *Biochemistry 17*, 5064−5070.
25. Englert, A., and Leclerc, M. (1978) *Proc. Natl. Acad. Sci. U.S.A. 75*, 1050−1051.
26. Cheung, H. C. (1991) in *Topics in Fluorescence Spectroscopy* (Lakowicz, J. R., Ed.) Vol *2*, pp 127−176, Plenum Publishing Corp., New York.
27. Chen, Y., Yang, J. T., and Martinez, H. M. (1972) *Biochemistry 11*, 4120−4131.
28. Mitchinson, C., Wilderspin, A. F., Trinnaman, B. J., and Green, N. M. (1982) *FEBS Lett. 146*, 87−92.
29. Bishop, J. E., Squier, T. C., Bigelow, D. J., and Inesi, G. (1988) *Biochemistry 27*, 5233−5240.
30. Pick, V., and Karlish, S. (1980) *Biochim. Biophys. Acta 626*, 255−261.
31. Pick, V., and Bassilian, S. (1981) *FEBS Lett. 123*, 127−136.
32. Gryczynski, I., Wiczk, W., Inesi, G., Squier, T., and Lakowicz, J. R. (1989) *Biochemistry 17*, 5064−5070.
33. Lakowicz, J. R., Johnson, M. L., Wiczk, W., Bhat, A., and Steiner, R. F. (1987) *Chem. Phys. Lett. 138*, 587−593.
34. Bevington, P. R., and Robinson, D. K. (1992) *Data reduction and error analysis for the physical sciences* (Second Edition), McGraw-Hill, New York.
35. Jorge-Garcia, I., Bigelow, D. J., Inesi, G., and Wade, J. B. (1988) *Arch. Biochem. Biophys. 265*, 82−90.
36. Bergenhem, N. C. H., Lee, S.-J., and Gafni, G. (1997) *JAGS 52A*, B240−B244.
37. Gafni, A. (1997) *JAGS 45*, 871−880.
38. Bigelow, D. J., and Thomas, D. D. (1987) *J. Biol. Chem. 262*, 13449−13456.
39. Bigelow, D. J., Squier, T. C., and Thomas, D. D. (1986) *Biochemistry 25*, 194−202.

40. Squier, T. C., Bigelow, D. J., and Thomas, D. D. (1988) *J. Biol. Chem. 263*, 9178−9186.
41. Cornea, R. L., and Thomas, D. D. (1994) *Biochemistry 33*, 2912−22920.
42. Krainev, A. G., Ferrington, D. A., Williams, T. D., Squier, T. C., and Bigelow, D. J. (1995) *Biochim. Biophys. Acta 1235*, 406−418.
43. Brandl, C. J., Green, N. M., Korczak, B., and Maclennan, D. H. (1986) *Cell 44*, 597−607.
44. Viner, R. I., Ferrington, D. A., Williams, T. D., Bigelow, D. J., and Schoneich, C. (1999) *Biochem. J. 340*, 657−669.
45. Wickler, S. J. (1981) *Am. J. Physiol. 241*, R185−R189.
46. Dumonteil, E., Barre, H., and Meissner, G. (1995) *Am. J. Physiol. 269*, C955−C960.
47. Duchamp, C., and Barre, H. (1993) *Am. J. Physiol. 265*, R1076−R1083.

BI991125N